
















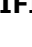




Equilibrium, Kinetic Data, and Adsorption Mechanism for Lead Adsorption onto Polyacrylamide Hydrogel

Imane LEBKIRI^{1,*}  , Brahim ABBOU¹  , Lamya KADIRI¹  ,
Abdelkarim OUASS¹  , Abdelhay ELAMRI¹  , Hanae OUADDARI²  ,
Omar ELKHATTABI¹  , Ahmed LEBKIRI¹  , El Housseine RIFI¹  

¹Laboratory of Advanced Materials and Process Engineering, Faculty of Sciences, Ibn Tofail University – Kenitra – Morocco.

²Laboratory of Materials Membranes and Environment, Department of Chemistry, Faculty of Sciences and Technologies of Mohammedia, University of Hassan II, Casablanca, Morocco.

Abstract: The present study focuses on the effect of experimental parameters (pH, temperature, gel mass, metal concentration, contact time) on the performance of lead adsorption by polyacrylamide hydrogels. The results obtained showed that the retention of Pb²⁺ ions is closely linked to these parameters. The adsorbent gels equilibrate with the metal solution after 180 minutes, and the maximum adsorption capacity is 442.31 mg/g. In addition, the adsorption obeys the pseudo-second-order kinetics and Langmuir isotherm. Desorption of the micropollutant retained by the hydrogel was also studied using 0.1 M of HCl solution. The desorption was rapid, and the efficiency exceeded 90% after a contact time of 90 minutes.

Keywords: Adsorption, lead, water treatment, hydrogel, polyacrylamide.

Submitted: April 09, 2021. **Accepted:** June 15, 2021.

Cite this: Lebkiri I, Abbou B, Kadiri L, Ouass A, Elamri A, Ouaddari H, et al. Equilibrium, Kinetic Data, and Adsorption Mechanism for Lead Adsorption onto Polyacrylamide Hydrogel. JOTCSA. 2021;8(3):731-48.

DOI: <https://doi.org/10.18596/jotcsa.912479>.

***Corresponding author.** E-mail: imane.lebkiri@gmail.com

INTRODUCTION

It is well known that heavy metals such as cadmium, lead, copper, and mercury are toxic to humans and other living organisms when their concentration exceeds the tolerance limit. Unlike organic contaminants, heavy metals are not biodegradable and accumulate in living organisms. Heavy metals are increasingly being released, either directly or indirectly, into the environment, particularly in developing countries (1).

Our attention has been focused on lead, which is considered one of the toxic metals that accumulate

slowly in living organisms from the food chain and has several harmful effects on human health (2).

Eliminating these types of pollutants is always a big challenge. Numerous studies have developed several treatment processes to reduce the amount of these contaminants in aquatic environments (3,4). The adsorption process is one of the methods that has shown outstanding cost-effectiveness in contaminants removal of a different nature, including organic pollutants and heavy metals (5,6). Besides, the research and development of new adsorbents, with a high capacity for adsorption, abundant, economically profitable, and effective for treating wastewater is

a great challenge. Thus, in recent years, a great importance has been attached to functionalized polymers because of their low cost and high capacity to adsorption different pollutants, especially the possibility of their regeneration (7-9).

Through the literature, polyacrylamide (PAAM) is one of the most widely used polymers (10,11). This material can absorb large amounts of water compared to other polymers (12). Polyacrylamide is a functionalized polymer containing a large number of amide groups that grant an excellent selectivity for the elimination of several organic pollutants and minerals (13). Due to its low cost, recoverable, eco-friendly, high adsorption capacity, and its use without any modification, PAAM can be a great adsorbent for heavy metal removal from wastewater (14,15). Moreover, one of the essential advantages of using this polymer is its structure containing abundant active sites that can fix metal species. Also, the shape and the mechanical rigidity of the adsorbent promote the separation procedure at the end of the adsorption experience. Various studies have investigated the PAAM hydrogel as a heavy metals adsorbent, such as the removal of mercury ions from aqueous solutions by Ramadan et al. (2010) (16); the removal of chromium ions from industrial lean methyl diethanolamine solvents (MDEA) by Pal and Banat (2015) (17) and the copper adsorption by S. Moulay et al. (2013) (18).

This work aims to study the effect of the physical-chemical parameters linked on the one hand to metallic solution and on the other hand to the polymeric matrix. The optimization of these parameters allows defining the amount of gel needed to treat a given metal solution volume. The equilibrium data were analyzed using various adsorption isotherms and kinetics.

EXPERIMENTAL SECTION

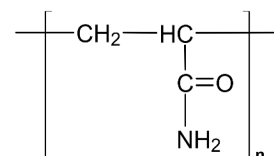
Adsorbate

The stock solution of lead is prepared from the corresponding salt: $Pb(NO_3)_2$ supplied by the company SOLVACHIM (Casablanca, Morocco). The solution studied is prepared by successive dilutions of the stock solution until the desired concentration is obtained.

Adsorbent

The material used in this work is polyacrylamide (PAAM), whose chemical formula is $([-C_2H_3CONH_2-])_n$ (Figure 1). It's a polymer made by radicalic polymerization of acrylamide and bisacrylamide. PAAM is a superabsorbent hydrogel with transparent beads of non-porous surface aspect supplied by Sigma-Aldrich (Saint Louis,

USA) (CAS number: 9003-05-8, purity: 99.99%, MW: 150000).



Adsorption Experiments

The adsorption experiments were carried out in a static regime in a stirred reactor at a fixed temperature ($25 \text{ }^\circ\text{C} \pm 2 \text{ }^\circ\text{C}$). The system was adjusted to the desired pH by adding small volumes of 0.01 or 0.1 mol/L HCl, or NaOH supplied by the company SOLVACHIM (Casablanca, Morocco). The quantities of metal adsorbed and the metal removal efficiency was calculated from the concentrations in the solutions, before and after adsorption according to the following equations (19,20):

$$Q = \frac{C_i - C_f}{m} * V \quad (\text{Eq. 1})$$

$$R\% = \frac{(C_i - C_f)}{C_i} * 100 \quad (\text{Eq. 2})$$

Where: Q is the adsorbed amount of lead at equilibrium (mg/g), R% is the lead removal efficiency (%), C_i and C_f , respectively, the initial and equilibrium lead concentration (mg/L), m is the mass of adsorbent (g) and V the volume of the lead solution (L).

The FT-IR spectra were obtained by 70 Vertex instrument of Bruker brand. The analysis was done by scanning from 4000 cm^{-1} to 400 cm^{-1} with a resolution of 4 cm^{-1} . X-ray diffraction analyses were recorded using a PANalytical X'Pert HighScore Plus diffractometer using Cu-K α radiation (1.5418 \AA) at a goniometer rate of $2\theta = 4^\circ/\text{min}$. SEM analysis was carried out using QUATTRO S, FEI. The heavy metal content analysis was carried out by optical emission spectrometry coupled to inductive plasma ICP-OES (Ultima2, Horiba Jobin Yvon).

Desorption Experiments

To assess the regenerative property of our adsorbent PAAM, HCl was tested as an eluent (supplied by the company SOLVACHIM (Casablanca, Morocco)). The gels loaded with lead are each immersed in 40 mL of a 0.1 M HCl solution. The experiment was stirred and performed at $25 \text{ }^\circ\text{C}$. Then the PAAM beads were collected from the solution, washed with distilled

water to remove acid excess acid, neutralized with 0.1 M NaOH, and washed again to remove NaOH excess. Then the beads were reused in the next cycle of the adsorption experiment. The adsorption-desorption experiments were carried out for five cycles.

Model to Experimental Data

- Adsorption kinetics analysis was calculated using (21):
The pseudo-second-order rate equation as (22):

The pseudo-first-order rate equation as (23):

$$\frac{dQ_t}{dt} = K_2(Q_e - Q_t)^2 \Rightarrow \frac{t}{Q_t} = \frac{1}{K_2 Q_e^2} + \frac{1}{Q_e} t \quad (\text{Eq. 3})$$

$$\frac{dQ_t}{dt} = K_1(Q_e - Q_t) \Rightarrow \ln(Q_e - Q_t) = \ln Q_e - K_1 t \quad (\text{Eq. 4})$$

Where K_1 is the pseudo-first-order rate constant (g/mg min), K_2 is the pseudo-second-order rate constant (g/mg min), Q_e and Q_t are the metal uptake (mg/g) at equilibrium and at time t , respectively.

- The Freundlich sorption isotherm equation is given below (24):

$$Q = K_f \frac{C_e^1}{n} \Rightarrow \log(Q) = \log(k_f) + \frac{1}{n} \log(C_e) \quad (\text{Eq. 5})$$

Where K_f (mg/g) represents the adsorption capacity, and n represents the degree of dependence of adsorption with equilibrium concentration.

The Langmuir sorption isotherm equation is given below (25):

$$Q_t = Q_m \frac{K_L C_e}{1 + K_L C_e} \Rightarrow \frac{C_e}{Q_t} = \frac{1}{K_L Q_m} + \frac{C_e}{Q_m} \quad (\text{Eq. 6})$$

Furthermore, the separation factor (R_L) was used to determine whether the adsorption was favorable or not. The R_L was calculated from the following equation:

$$R_L = \frac{1}{1 + K_L C_0} \quad (\text{Eq. 7})$$

Where C_0 and C_e represent the initial and equilibrium concentration of heavy metals (mg/L); Q_m is the adsorption capacity (mg/g), and K_L is related to the energy of adsorption (L/mg).

For the thermodynamic studies, the Eyring equation was used (26):

$$\ln K_d = \left(\frac{\Delta S}{R} \right) - \left(\frac{\Delta H}{R} \right) \frac{1}{T} \quad \text{and} \quad (\text{Eq. 8})$$

$$\Delta G = -RT \ln K_d \ln K_d = \left(\frac{\Delta S}{R} \right) - \left(\frac{\Delta H}{R} \right) \frac{1}{T}$$

Where $K_d = Q_e / C_e$ is the sorption distribution constant and Q_e the adsorption capacity at equilibrium (mg/g), and C_e is the amount of Pb^{2+} in solution at equilibrium (mg/L), R ideal gas constant (8,314 J.mol⁻¹.K⁻¹) and T the temperature (K), ΔG° is the Gibbs free energy (J/mol), ΔS the entropy (J/kmol) and ΔH the enthalpy (J/mol).

RESULTS AND DISCUSSION

Characterization of PAAM

X-ray diffraction

X-ray diffraction makes it possible to determine the structure of the polymer studied. Figure 2 shows the X-ray diffraction pattern of the polymer in powder form. The absence of peaks in this figure's spectrum shows that the polymer studied is an amorphous product (27,28).

FTIR spectroscopy of PAAM

An infrared spectroscopic (IR) study of PAAM gels before and after lead adsorption was performed (Figure 3). The purpose of this study is to understand the mechanism of fixation of Pb^{2+} ions by polyacrylamide. The study is based on the comparison of the spectra of free and doped lead polymers.

The spectrum of blank PAAM shows two peaks at 3465.44 cm⁻¹ due to the valence vibration of the amino group N-H stretching (primary amine) (29–31). The absorption peak at 2923 cm⁻¹ could be attributed to the C-H elongation vibration of the CH₂ group. The adsorption peak at 1639 cm⁻¹ confirms the presence of C=O and that at 1382 cm⁻¹ corresponds to the valence vibration of C-N, whereas that at 998 cm⁻¹ and 622 cm⁻¹ corresponds to the valence vibration of NH₂ (32–34).

The first change observed after lead adsorption appears at the peaks corresponding to the N-H vibration; they become wider and intense with the appearance of a new band of N-H at 1561.44 cm⁻¹. A bending vibration is observed at 1615 cm⁻¹ corresponding to the double band C=O; after the adsorption of the lead, this band becomes more intense. The vibration bands C-H, CH₂, and C-N, do not change the spectra of the formed complex. They are therefore not involved in the coordination of Pb^{2+} to the PAAM polymer.

The observations presented above show that PAAM probably acts as a bidentate ligand, coordinating with the metal Pb^{2+} center by two bonds to the CO and NH_2 groups (Figure 4). This coordination leads

to a chemical crosslinking of the polymer and thus the repulsion of the water molecules present in the polymer network. This explains the deflation of the gel after lead adsorption (35).

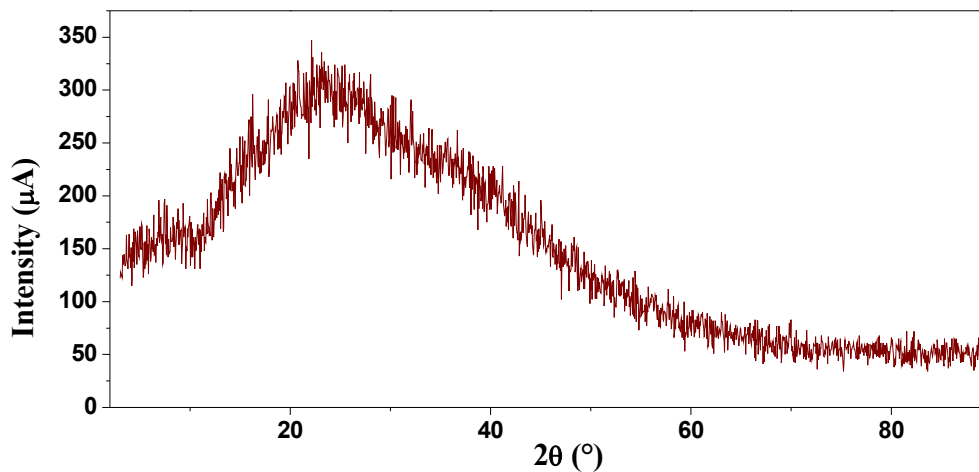


Figure. 2: X-ray diffraction of PAAM.

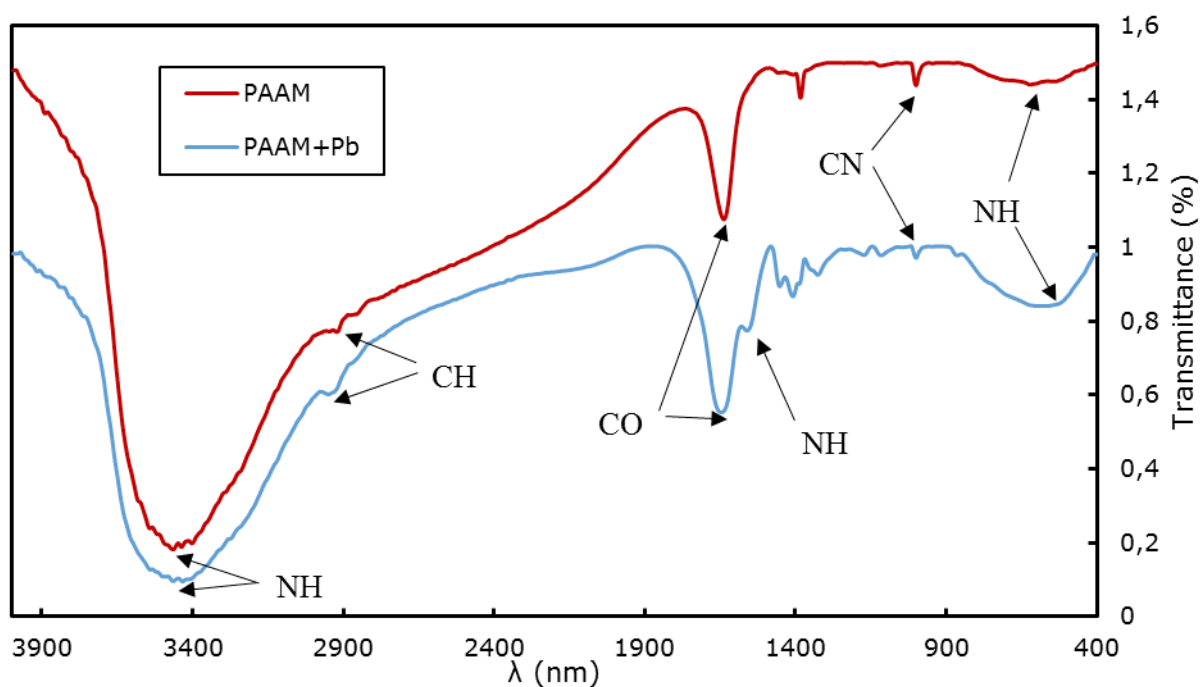


Figure 3: IR spectrometry of PAAM hydrogel and lead charged PAAM.

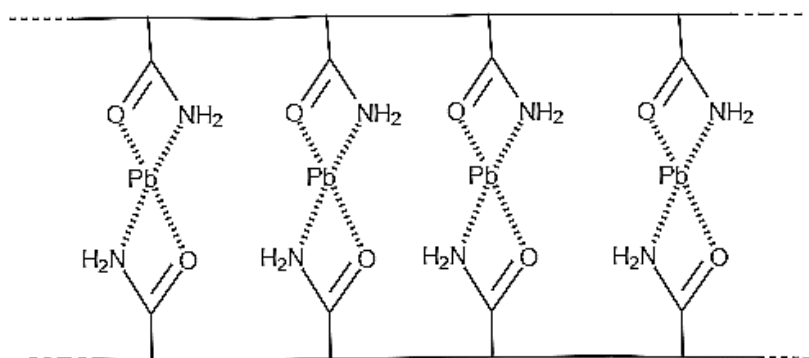


Figure 4: PAAM-Pb complex.

SEM analysis

Figure 5 (a) shows the SEM micrograph of the lead-containing gel, and Figure 5 (b) shows the EDX mapping of the region shown in (a), the lead, shown in turquoise blue, is present in the gel in a random distribution. Figure 5 (c) shows the EDX spectrum of the same region and peaks are corresponding to Pb, N, and O; these last two elements should be present in a PAAM polymer; carbon is detected, but this corresponds to the carbon in the gel and the carbon ribbon. Pb peak is present; it confirms the presence of lead on the gel (36).

Effects of Different Experimental Parameters on Adsorption of Lead by PAAM

Effect of contact time

Experiments were performed to determine the time required for the metal removal process to reach equilibrium. The study consists of placing, in a temperature-controlled cell, a volume of 100 mL of 20 ppm of lead solution and 0.026 g of PAAM gel. The whole is stirred at 25 °C until equilibrium. The following curve represents the simultaneous variations of the concentration and the pH of the metallic solution versus time.

According to Figure 6, we notice two phases: the first one is fast from 0 to 30 minutes, and the second phase is slow from 60 until 180 minutes when equilibrium is reached. This is relating to the wide availability of the free active sites of PAAM at the beginning of the experience, which becomes weak over time (37).

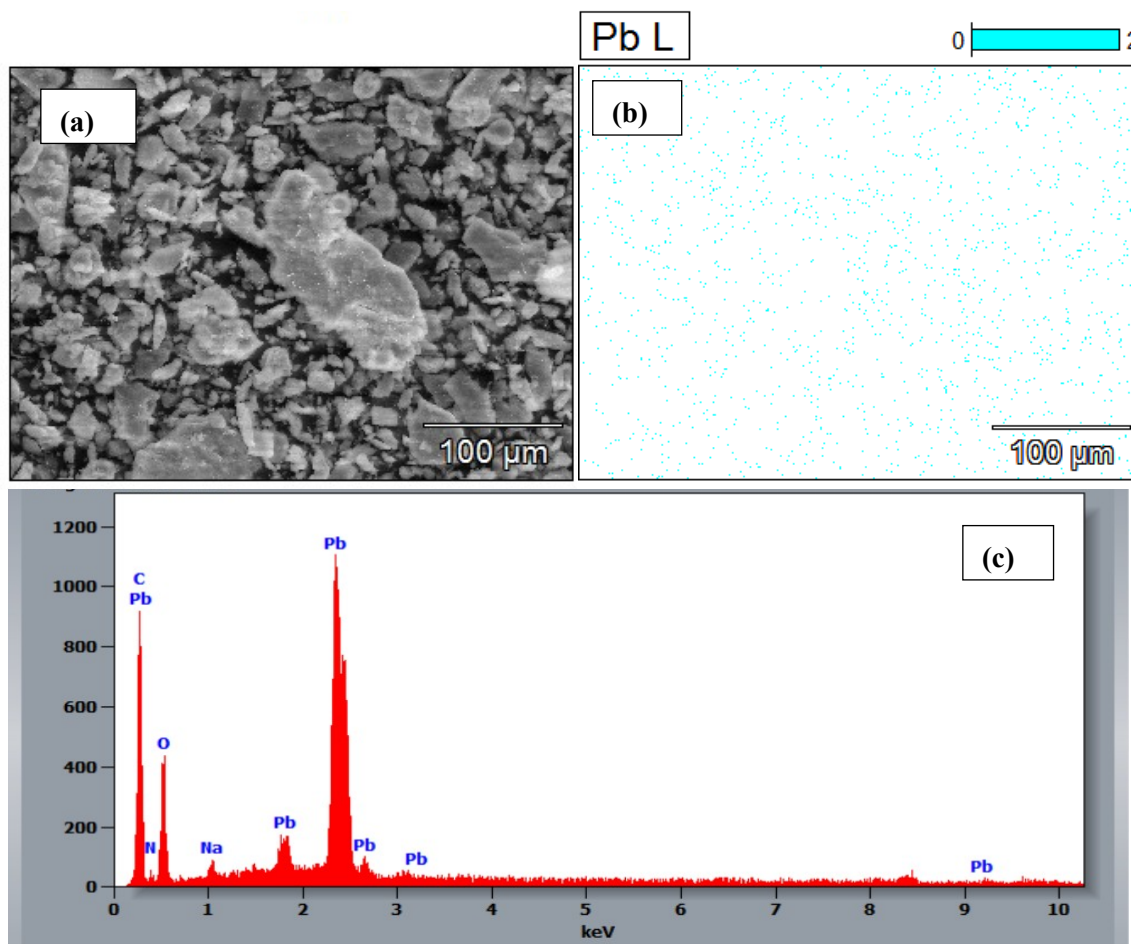


Figure 5: EDX analysis coupled with the SEM of the lead-laden PAAM

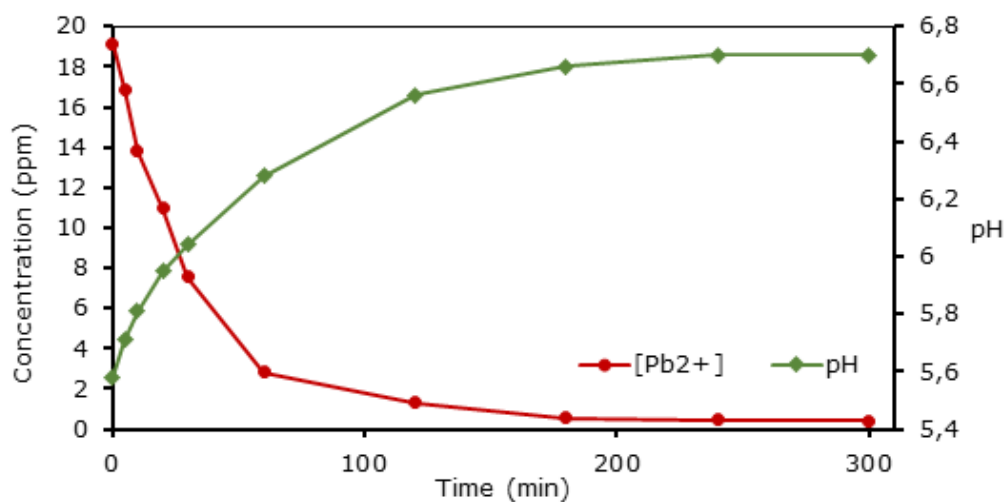


Figure 6: Evolution of lead concentration and pH over time (V=100 mL, T=25 °C, pH=5, m=0.026 g, [Pb²⁺]=20 ppm).

At the same time, we observe an increase in the pH, ranging from 5.5 to 6.7. The increase in pH shows that the gel equilibrates with the solution

loaded with metal by consuming H⁺ (19). In our operating conditions, we record an adsorption efficiency close to 97%.

Effect of adsorbent dose

Studying the effect of PAAM's mass on lead adsorption allows us to determine the optimal mass that will be used throughout our study. For this purpose, we put PAAM masses varying from 0.007 to 0.08 g each in contact with 100 mL of metal solution. The results obtained are shown in Figure 7. According to the results, the percentage of lead elimination by PAAM increases rapidly with the increase in the mass of the adsorbent to the value of 0.026 g. Beyond this value, the increase in adsorbent content slightly affects the adsorption of the lead until reaching an equilibrium of 100%. This is explained by the fact that by adding the adsorbent, more active centers will be available to adsorb Pb^{2+} ions. Therefore the system reaches an equilibrium state for an initial lead concentration of 20 ppm (38). Finally, 0.026 g will be considered and used as optimal mass.

Effect of pH

pH has a remarkable influence on the process of removing metal cations in aqueous solutions by adsorption, as it directly affects the surface load and the nature of the ion species of adsorbates. In this context, the effect of pH on the adsorption of lead by PAAM gel was studied at different values: 2, 3, 4, 5, and 6. Masses of PAAM are put in contact with lead solutions. According to Figure 8, it can be observed that the adsorption efficiency of lead increases with increasing pH. Indeed, at acidic pH, the adsorption yield is almost equal to 16%, and it increases with increasing pH until reaching a

maximum corresponding to equilibrium at pH = 4, where the yield is equal to 97% (39). This can be explained by the fact that at low pH values, the surface of the adsorbent would be surrounded by H^+ , which would decrease the interaction of Pb^{2+} with the sites of the adsorbent due to repulsive forces. The decrease in adsorption at low pH values may be due to the high concentration and high mobility of the H^+ , which are preferentially adsorbed than metal ions (40). On the other hand, the gels' deflation at a more acidic pH prevents the diffusion of metal ions in the gel. With the increase in pH, the quantity of protons in solution decreases, the competition between H^+ and Pb^{2+} for the occupation of surface sites becomes less strong, hence increasing adsorption yield.

Effect of the temperature

Temperature is a significant parameter in the adsorption process. To study the influence of this parameter, experiments were carried out at different temperatures (25, 35, 45, and 55 °C) using a thermostat. The resulting mixture was stirred until equilibrium. Figure 9 represents the effect of temperature in the performance of lead adsorption by the PAAM. Based on the results obtained, we find that the increase in temperature causes an increase in the adsorption efficiency (41). In fact, the increase in temperature leads to the expansion of the polymer's macromolecular chain, promoting the metal's adsorption. These results show that the adsorption process is probably endothermic.

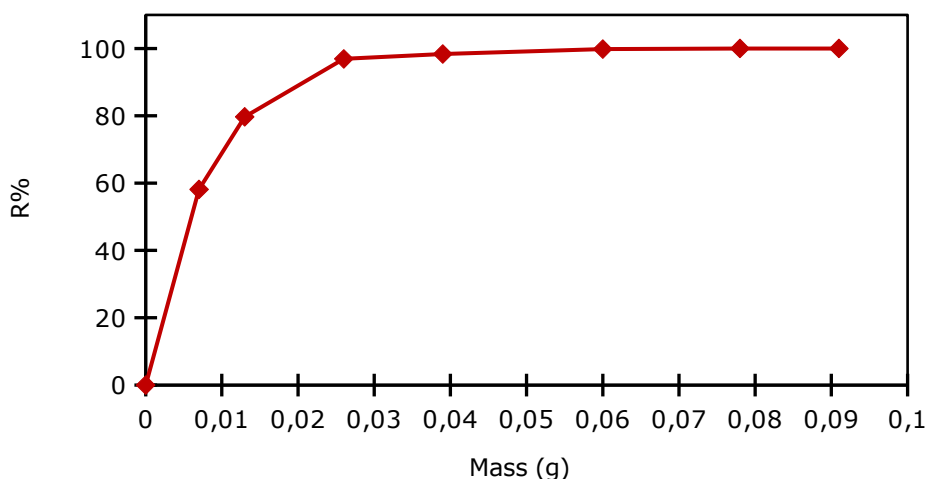


Figure 7: Effect of the mass of the PAAM polymer on the adsorption of lead ($T=25\text{ }^{\circ}\text{C}$, $[Pb^{2+}]=20\text{ ppm}$, $pH=5$, $t=3\text{ h}$, $V=100\text{ mL}$).

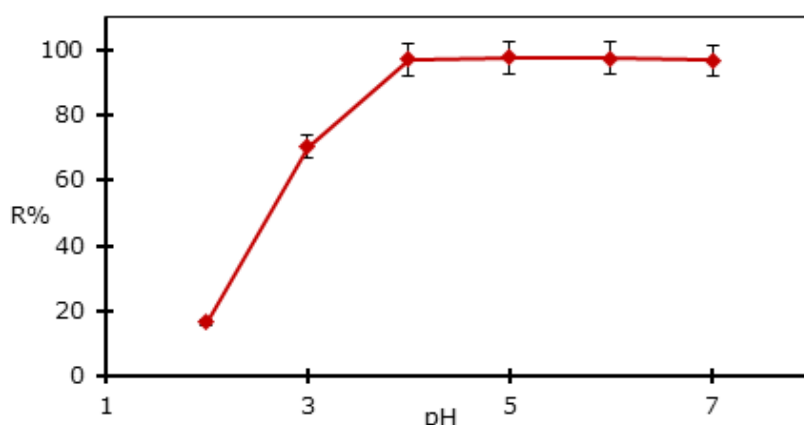


Figure 8: Effect of the pH on adsorption lead by PAAM (T=25 °C, m=0.026 g, V=100 mL, [Pb²⁺] =20 ppm).

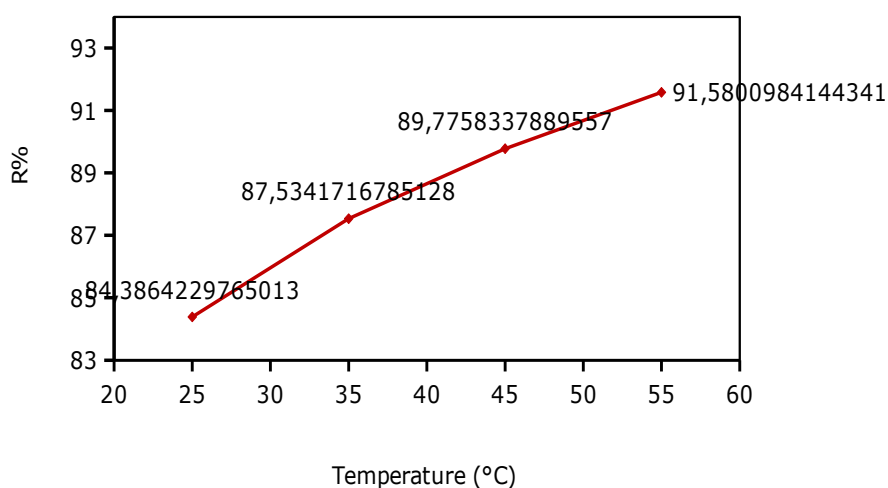


Figure 9: Effect of the temperature on lead adsorption by PAAM (m=0.026 g, V=100 mL, pH=5, [Pb²⁺]=20 ppm, t =3 h)

Effects of ionic strength

The effect of ionic strength on the sorption of lead ions onto PAAM was studied by conducting experiments at different concentrations of NaCl (25, 50, 100, 200, and 300 mg/L) (Figure 10). We observe from the figure that the amount of Pb ions

decreased with an increase in the ionic strength of the electrolyte solution. This can be explained, probably, by the competition of lead ions with other ions to adhere with the adsorbent. This result is confirmed by previous work concerned with water treatment (42,43).

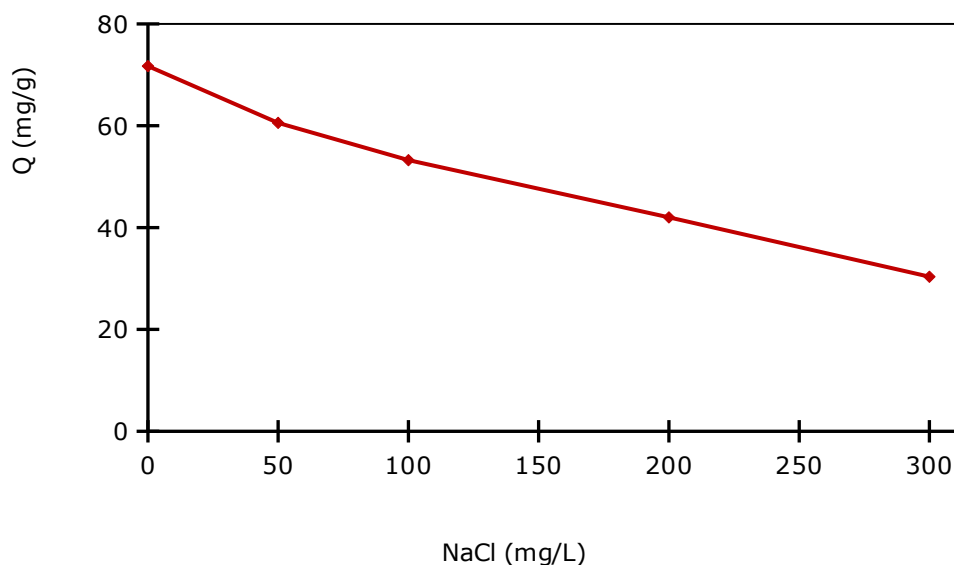


Figure 10: Effect of various ionic strength on lead adsorption by PAAM ($m=0.026$ g, $V=100$ mL, $T= 25$ °C, $pH=5$, $[Pb] = 20$ ppm, $t=3$ h).

Effect of the initial lead concentration

The initial concentration of the pollutant has an important influence on the retention capacity of the support. To study its effect, solutions of lead at different concentrations: 20, 50, 100, 150, 200, 300, and 500 ppm were considered. It appears from Figure 11 that the initial concentration of the metal actually influences the retention process. Indeed, the ability to fix the ions increases as the lead solution's content increases. A maximum is

obtained for a concentration close to 200 ppm, where the retention capacity of lead reaches 442.31 mg/g. This can be explained by the depletion of all existing active sites at the surface of the support (44). Besides, the increase in concentration induces the increase in the driving force of the concentration gradient, thus increasing the diffusion of dye molecules in solution through the surface of the adsorbent (45).

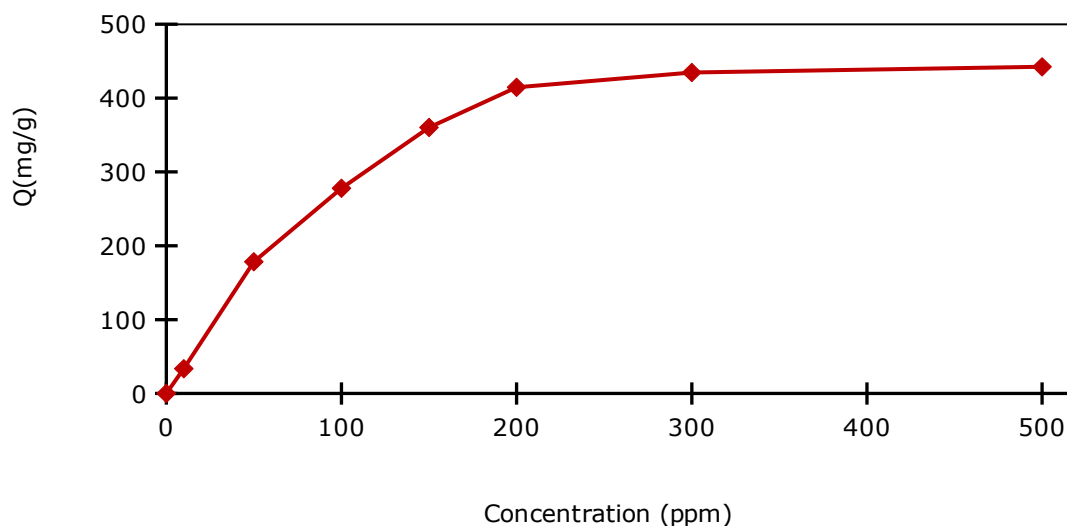


Figure 11: Adsorption capacity versus the initial lead concentration.

Isotherms and Kinetics of Lead Adsorption by PAAM

Adsorption isotherm

The adsorption capacity of lead by PAAM gels was studied as a function of the initial lead

concentration. The experimental conditions are identical to those used previously. The initial concentration of lead varies from 20 to 500 ppm. The results obtained were modeled by two empirical models: Langmuir and Freundlich. These

two models provide a widely used tool for elucidating the adsorption mechanism and quantifying adsorbent/adsorbate affinity.

Figure 12 (a, b) represents the isotherms of lead adsorption by PAAM. It is observed that the adsorption is satisfactorily described by the Langmuir model ($R^2 = 0.9994$), reflecting the homogeneous nature of the surface of this solid (PAAM).

Table 1 represents the various parameters calculated from the Langmuir and Freundlich

models. According to these results, it can be seen that the maximum adsorbed quantity obtained by the Langmuir model 454.54 mg/g is very close to that obtained experimentally 442.31 mg/g, the correlation coefficient $R^2 = 0.9994$ is close to unity, and the separation factor $R_L < 1$ implying that the adsorption of lead on PAAM is favorable (46). This reinforces the validity of the Langmuir model, which is based on monolayer coverage and the absence of interactions between the entities adsorbed on sites of the same nature. These results agree with previous work on other supports loaded with Pb, cited in the literature (47,48).

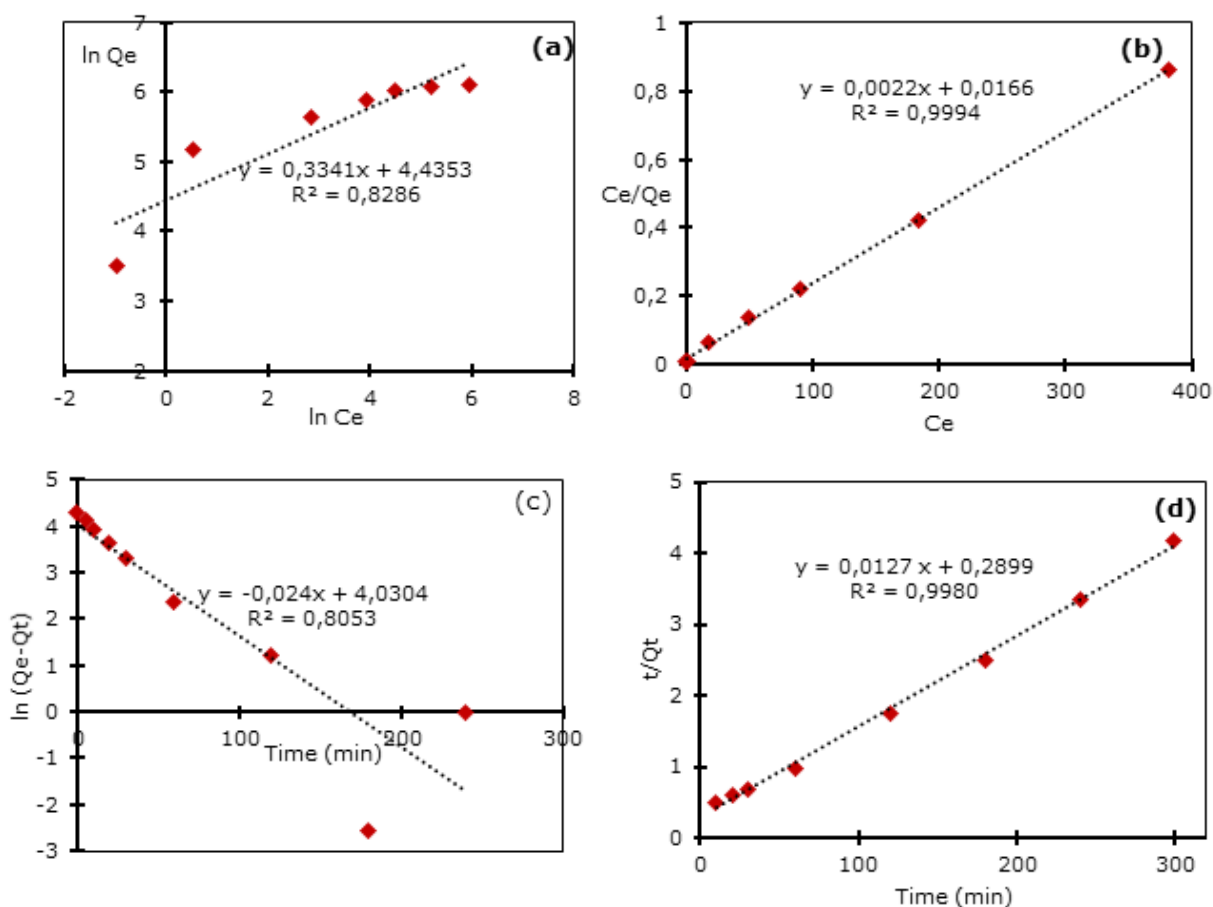


Figure 12: Freundlich (a), Langmuir (b) isotherms and Pseudo-first-order (c), Pseudo second-order (d) kinetics applied to lead²⁺ ion adsorption by PAAM.

Adsorption kinetics

Two kinetic models were applied to describe the mechanism of lead adsorption by PAAM gels: Pseudo first-order kinetic model and pseudo second-order kinetic model (Figure 12 c, d). The purpose of applying these models is to provide general expressions capable of describing the adsorption kinetics of solutes on a surface.

Table 2 represents the various kinetic parameters calculated from the graphic representation of these models. The calculated kinetic parameters are K1, K2, and Qe (adsorption quantity) for both models. The value of the amount of lead adsorption calculated from the pseudo-second-order model is the closest to that determined experimentally, which indicates the suitability of using this model to describe the adsorption of lead by PAAM. The

correlation coefficient of the pseudo-second-order model is of the order of 0.998. For the pseudo-first-order model, the correlation coefficient is 0.8053. These data confirm that the pseudo-second-order kinetic model is the most reliable to describe the adsorption of lead by PAAM. This model suggests that the lead adsorption depends on the adsorbate and the adsorbent and that a chemisorption process is involved in this sorption and physisorption. This is in good agreement with previous work on other supports loaded with Pb, cited in the literature (49,50).

Thermodynamic study

Determining thermodynamic parameters is very important to understand the effect of temperature

on adsorption better. In principle, it can also predict the strength of the bonds between the adsorbent and the adsorbate.

Figure 13 shows the $\ln K_d=f(1/T)$ curve for the adsorption of lead by PAAM. The thermodynamic parameters of this process are shown in Table 3. The standard enthalpy value is positive, which confirms that the adsorption process is endothermic. It is accepted that the binding energies of physical adsorption are generally between -20 and 0 kJ/mol, while the energies of a chemical bond are in the range of -80 to -400 kJ/mol (51). In our case, the enthalpy is equal to 18 kJ/mol, which means that the adsorption of lead by PAAM is physical in nature.

Table 1: Parameters of the Langmuir and Freundlich equations for lead adsorption by PAAM.

Langmuir isotherm				Freundlich isotherm			
$Q_{m, exp}$ (mg/g)	Q_m (mg/g)	K_L (L/mg)	R^2	R_L	K_f (mg/g)	$1/n$	R^2
442.32	454.54	0.13	0.9994	0.453-0.0149	84.37	0.3341	0.8286

Table 2: Kinetics parameter of lead adsorption by PAAM.

Pseudo-first-order				Pseudo-second-order		
Q_{max} (mg/g)	K_1 (g/mg.min)	Q_e (mg/g)	R^2	K_2 (g/mg.min)	Q_e (mg/g)	R^2
71.99	0.024	56.28	0.8053	0.00055461	78.86	0.9980

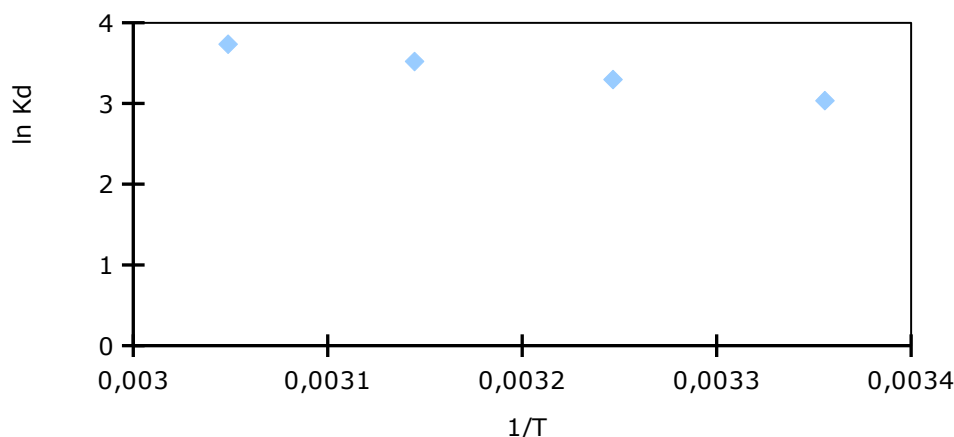


Figure 13: Van't Hoff plot of lead adsorption by PAAM.

Table 3: Thermodynamic parameters of lead adsorption by PAAM.

T (K)	ΔG (J/mol)	ΔH (J/mol)	ΔS (J/k,mol)	R^2
298	-7355.03			
308	-8257.65	18879.43	88.62	0.9996
318	-9103.93			
328	-9961.30			

Desorption of Lead Ions from PAAM

Among the characteristics and requirements that an adsorbent must have is its regeneration and reuse in adsorption. In fact, the adsorbents must be able to be regenerated by elution to recover the adsorbed metal. The results showed HCl is effective in removing the adsorbed metal. Figure 14 shows the adsorption and desorption yields of

metals during the five cycles of adsorption-desorption. It can be seen that the rate of desorption was generally above 97%, and the adsorption efficiency was hardly affected. These results indicate that the polyacrylamide beads would have great potential in practical applications for the removal of metal ions as well as for their recovery.

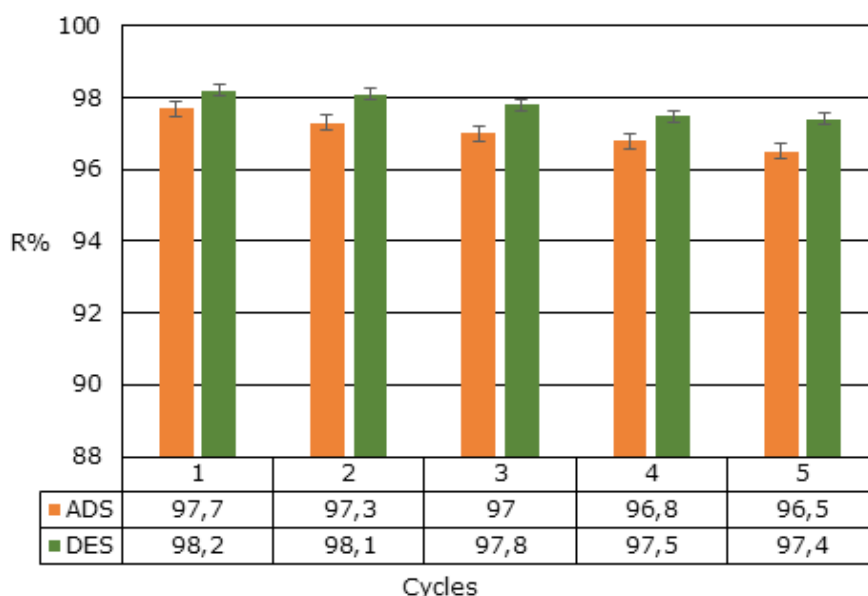


Figure 14: Adsorption and desorption of lead by PAAM.

To better visualize the desorption process, samples were taken from the HCl solution during desorption, diluted, and then dosed. Changes in the concentration of lead over time are shown in Figure 15. The equilibrium is reached at approximately 90 minutes, which shows that the desorption kinetics is 2 times faster than the adsorption kinetics. This can be explained by the low swelling of the metal-laden PAAM, which decreases the path traveled inside the gel and accelerates the diffusion of species during desorption.

Adsorption of Bivalent Cations by PAAM

To study the adsorption of other metals by PAAM, we introduced a magnitude of 0.026 g of PAAM gel in Pb^{2+} , Cd^{2+} , and Cu^{2+} solutions with the same concentration (10^{-4} M) (Figure 16). The curves obtained show quick adsorption for the three ions for the first 30 minutes. However, the equilibrium

is reached after 3 hours of contact regardless of the adsorbed metal. The maximum adsorption amounts reached are 71.6 mg/g, 46.8 mg/g and 28 mg/g of Pb^{2+} , Cu^{2+} and Cd^{2+} , respectively. It is clear that the PAAM adsorb Pb ions more than other metallic ions. These results can be attributed to the affinity of the polymeric hydrogel vis-a-vis certain metals; in fact, it can be influenced by the valency and the ionic size of the heavy metals once hydrated (52,53). At equal valence, a low-hydrated cation has more affinity than a high-hydrated cation. The smaller the non-hydrated radius of a cation, the stronger its hydrated radius, because it attracts water molecules more strongly. At equal valence, therefore, it is the voluminous cations that will be fixed preferentially and lead ions are voluminous, more than copper and cadmium, that's why they are more adsorbed by the adsorbent.

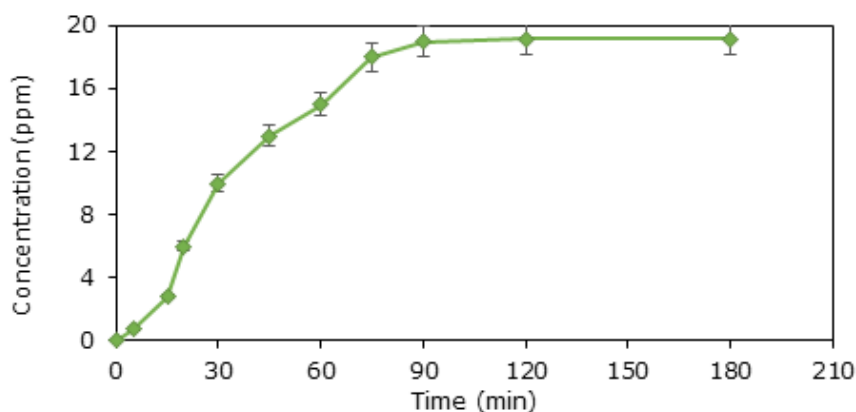


Figure 15: Kinetics desorption of lead by PAAM using HCl as eluent.

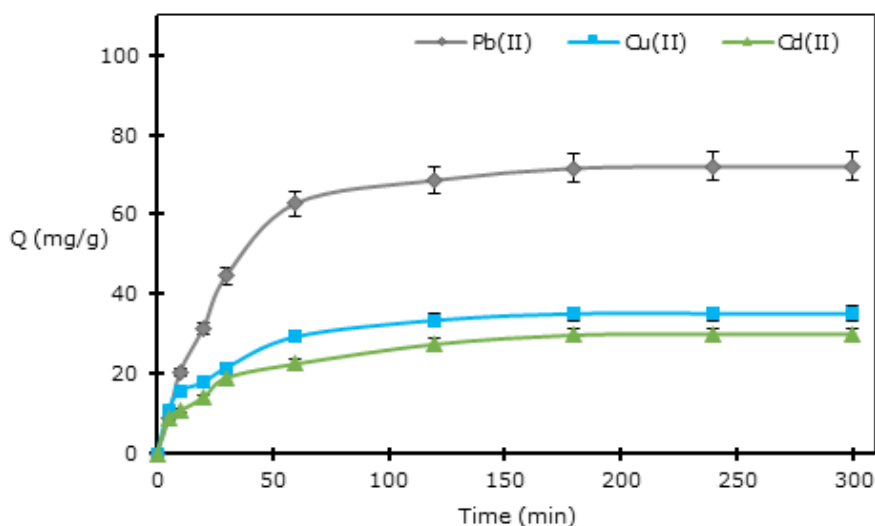


Figure 16: Absorption capacity of divalent cations by PAAM versus time.

Comparison with Other Adsorbents

It is found that the adsorption amount of PAAM among the highest capacities of hydrogels, and herein lies the novelty and the importance of using

PAAM hydrogel in heavy metal adsorption. Table 4 has shown various hydrogels that have been studied previously for the removal of Pb ions.

Table 4: Comparative study of the adsorption of PAAM by different hydrogels.

Adsorbent	Adsorption capacity (mg/g)	Reference
Chitosan hydrogel beads	124.2	(54)
Poly(N-isopropylacrylamide-co-benzo18-crown-6-acrylamide)	142	(55)
bentonite/ sodium lignosulfonate graft-polymerized with acrylamide and maleic anhydride (BLPAMA)	218.04	(56)
Acid hydrolysis lignin-g-poly-(acrylic acid)	235	(57)
poly (acrylamide-co-itaconic acid)/multi-walled carbon nanotubes (P(AAm-co-IA)/MWCNTs)	107.36	(58)
Polyacrylamide	442.31	Present work
poly (AA)-bentonitesuperabsorbent composites (SAC)	1666.67	(59)

CONCLUSION

Given the intense interest in superabsorbent polymers in recent years, we tested the potential of polyacrylamide to adsorb lead. The study of the influence of the experimental parameters showed that the equilibrium was reached after 180 minutes, and the decrease in the concentration of lead was accompanied by an increase in the pH of the solution, which implies that the gel equilibrates with the metal solution by fixing H⁺ protons. The increase in pH promoted the adsorption of the metal; a maximum was reached from pH = 4. At high lead concentrations, the gel reached its maximum metal load, about 442.31 mg/g.

Adsorption isotherm was studied on the considered concentration interval where the Langmuir model well represents experimental data. Linear representations of kinetic curves have shown that the pseudo-second-order model gives the best match compared to the pseudo-first-order.

ACKNOWLEDGMENT

The authors gratefully acknowledge the Technical Support Units for Scientific Research (UATRS) under the National Center for Scientific and Technical Research (CNRST), especially to Hanae OUADDARI for the analytical services and instrumentations.

REFERENCES

1. Burakov AE, Galunin EV, Burakova IV, Kucherova AE, Agarwal S, Tkachev AG, et al. Adsorption of heavy metals on conventional and nanostructured materials for wastewater treatment purposes: A review. *Ecotoxicology and Environmental Safety*. 2018 Feb;148:702–12. DOI: <https://doi.org/10.1016/j.ecoenv.2017.11.034>.
2. Boudrahem F, Aissani-Benissad F, Soualah A. Adsorption of Lead(II) from Aqueous Solution by Using Leaves of Date Trees As an Adsorbent. *J Chem Eng Data*. 2011 May 12;56(5):1804–12. DOI: <https://doi.org/10.1021/je100770j>.
3. Akpor O, Muchie M. Remediation of heavy metals in drinking water and wastewater treatment systems: Processes and applications. *Int J Phys Sci*. 2010;5(12):1807–17. DOI: <https://doi.org/10.5897/IJPS.9000482>.
4. Es-sahbany H, Berradi M, Nkhili S, Hsissou R, Allaoui M, Loutfi M, et al. Removal of heavy metals (nickel) contained in wastewater-models by the adsorption technique on natural clay. *Materials Today: Proceedings*. 2019;13:866–75. DOI: <https://doi.org/10.1016/j.matpr.2019.04.050>.

5. Dhir B, Kumar R. Adsorption of Heavy Metals by Salvinia Biomass and Agricultural Residues. *International journal of environmental research (IJER)*. 2010;4(3):427–32. URL: <https://www.sid.ir/en/Journal/ViewPaper.aspx?ID=182202>.

6. Es-sahbany H, Hsissou R, El Hachimi ML, Allaoui M, Nkhili S, Elyoubi MS. Investigation of the adsorption of heavy metals (Cu, Co, Ni and Pb) in treatment synthetic wastewater using natural clay as a potential adsorbent (Sale-Morocco). *Materials Today: Proceedings*. 2021;45:7290–8. DOI: <https://doi.org/10.1016/j.matpr.2020.12.1100>.

7. Siqueira DF, Reiter J, Breiner U, Stadler R, Stamm M. Competitive Adsorption of Functionalized Polymers. *Langmuir*. 1996 Jan;12(4):972–9. DOI: <https://doi.org/10.1021/la950519m>.

8. Huang Y, Zhao W, Zhang X, Peng H, Gong Y. Thiol-ene synthesis of thioether/carboxyl-functionalized polymers for selective adsorption of silver (I) ions. *Chemical Engineering Journal*. 2019 Nov;375:121935. DOI: <https://doi.org/10.1016/j.cej.2019.121935>.

9. Es-sahbany H, El Hachimi ML, Hsissou R, Belfaquir M, Es-sahbany K, Nkhili S, et al. Adsorption of heavy metal (Cadmium) in synthetic wastewater by the natural clay as a potential adsorbent (Tangier-Tetouan-Al Hoceima – Morocco region). *Materials Today: Proceedings*. 2021;45:7299–305. DOI: <https://doi.org/10.1016/j.matpr.2020.12.1102>.

10. Kim S, Iyer G, Nadarajah A, Frantz J, Spongberg A. Polyacrylamide Hydrogel Properties for Horticultural Applications. *Int J Polym Anal Character*. 2010 Apr;15(5):307–18. DOI: <https://doi.org/10.1080/1023666X.2010.493271>.

11. Kaşgöz H, Özgümüş S, Orbay M. Modified polyacrylamide hydrogels and their application in removal of heavy metal ions. *Polymer*. 2003 Mar;44(6):1785–93. DOI: [https://doi.org/10.1016/S0032-3861\(03\)00033-8](https://doi.org/10.1016/S0032-3861(03)00033-8).

12. Lira LM, Martins KA, Torresi SIC de. Structural parameters of polyacrylamide hydrogels obtained by the Equilibrium Swelling Theory. *European Polymer Journal*. 2009 Apr;45(4):1232–8. DOI: <https://doi.org/10.1016/j.eurpolymj.2008.12.022>.

13. Bertrand T, Peixinho J, Mukhopadhyay S, MacMinn CW. Dynamics of Swelling and Drying in a

- Spherical Gel. *Phys Rev Applied*. 2016 Dec;6(6):064010. DOI: <https://doi.org/10.1103/PhysRevApplied.6.064010>.
14. Moreno-Sader K, García-Padilla A, Realpe A, Acevedo-Morantes M, Soares JBP. Removal of Heavy Metal Water Pollutants (Co 2+ and Ni 2+) Using Polyacrylamide/Sodium Montmorillonite (PAM/Na-MMT) Nanocomposites. *ACS Omega*. 2019 Jun 30;4(6):10834–44. DOI: <https://doi.org/10.1021/acsomega.9b00981>.
15. Wiśniewska M, Fijałkowska G, Szewczuk-Karpisz K. The mechanism of anionic polyacrylamide adsorption on the montmorillonite surface in the presence of Cr(VI) ions. *Chemosphere*. 2018 Nov;211:524–34. DOI: <https://doi.org/10.1016/j.chemosphere.2018.07.198>.
16. Ramadan H, Ghanem A, El-Rassy H. Mercury removal from aqueous solutions using silica, polyacrylamide and hybrid silica-polyacrylamide aerogels. *Chemical Engineering Journal*. 2010 May 1;159(1-3):107–15. DOI: <https://doi.org/10.1016/j.cej.2010.02.051>.
17. Pal P, Banat F. Removal of Contaminants from Industrial Lean Amine Solvent Using Polyacrylamide Hydrogels Optimized by Response Surface Methodology. *Adsorption Science & Technology*. 2015 Jan;33(1):9–24. DOI: <https://doi.org/10.1260/0263-6174.33.1.9>.
18. Moulay S, Bensacia N, Garin F, Fechete I, Boos A. Polyacrylamide-Based Sorbents for the Removal of Hazardous Metals. *Adsorption Science & Technology*. 2013 Aug;31(8):691–709. DOI: <https://doi.org/10.1260/0263-6174.31.8.691>.
19. Ouass A, Essaadaoui Y, Kadiri L, Lebkiri I, Lafreme C, Cherkaoui M, et al. Adsorption of Cr (III) from aqueous solution by two forms of a superabsorbant polymer: parametric study and effect of activation mode. Boukdir A, El Mabrouki M, editors. *E3S Web Conf*. 2018;37:02001. DOI: <https://doi.org/10.1051/e3sconf/20183702001>.
20. Kadiri L, Lebkiri A, Rifi EH, Ouass A, Essaadaoui Y, Lebkiri I, et al. Kinetic studies of adsorption of Cu (II) from aqueous solution by coriander seeds (*Coriandrum Sativum*). Boukdir A, El Mabrouki M, editors. *E3S Web Conf*. 2018;37:02005. DOI: <https://doi.org/10.1051/e3sconf/20183702005>.
21. Lagergren S. Zur theorie der sogenannten adsorption gelöster stoffe. *Kungliga Svenska Vetenskapsakademiens Handlingar*. 1898;24(4):1–39.
22. Essaadaoui Y, Lebkiri A, Rifi EH, Kadiri L, Ouass A. Adsorption of cobalt from aqueous solutions onto Bark of Eucalyptus. *Mediterr J Chem*. 2018 Sep 15;7(2):145–55. DOI: <https://doi.org/10.13171/mjc72/01808150945-essaadaoui>.
23. Essaadaoui Y, Lebkiri A, Rifi E, Kadiri L, Ouass A. Adsorption of lead by modified Eucalyptus camaldulensis barks: equilibrium, kinetic and thermodynamic studies. *DWT*. 2018;111:267–77. DOI: <https://doi.org/10.5004/dwt.2018.22191>.
24. Freundlich H. Über die adsorption in lösungen. *Z Phys Chem*. 1907;57(1):385–470.
25. Huang J, Liu Y, Jin Q, Wang X, Yang J. Adsorption studies of a water soluble dye, Reactive Red MF-3B, using sonication-surfactant-modified attapulgite clay. *Journal of Hazardous Materials*. 2007 May;143(1-2):541–8. DOI: <https://doi.org/10.1016/j.jhazmat.2006.09.088>.
26. Chakir A, Bessiere J, Kacemi KEL, Marouf B. A comparative study of the removal of trivalent chromium from aqueous solutions by bentonite and expanded perlite. *Journal of Hazardous Materials*. 2002 Nov;95(1-2):29–46. DOI: [https://doi.org/10.1016/S0304-3894\(01\)00382-X](https://doi.org/10.1016/S0304-3894(01)00382-X).
27. Baron RI, Bercea M, Avadanei M, Lisa G, Biliuta G, Coseri S. Green route for the fabrication of self-healable hydrogels based on tricarboxy cellulose and poly(vinyl alcohol). *International Journal of Biological Macromolecules*. 2019 Feb;123:744–51. DOI: <https://doi.org/10.1016/j.ijbiomac.2018.11.107>.
28. Kadiri L, Lebkiri A, Rifi E, Essaadaoui Y, Ouass A, Lebkiri I, et al. Characterization of coriander seeds "coriandrum sativum." *International Journal of Scientific and Engineering Research*. 2017;8(7):2303–8.
29. Yuan N, Xu L, Zhang L, Ye H, Zhao J, Liu Z, et al. Superior hybrid hydrogels of polyacrylamide enhanced by bacterial cellulose nanofiber clusters. *Materials Science and Engineering: C*. 2016 Oct;67:221–30. DOI: <https://doi.org/10.1016/j.msec.2016.04.074>.
30. Liu R, Liang S, Tang X-Z, Yan D, Li X, Yu Z-Z. Tough and highly stretchable graphene oxide/polyacrylamide nanocomposite hydrogels. *J Mater Chem*. 2012;22(28):14160. DOI: <https://doi.org/10.1039/c2jm32541a>.

31. Zhou C, Wu Q, Lei T, Negulescu II. Adsorption kinetic and equilibrium studies for methylene blue dye by partially hydrolyzed polyacrylamide/cellulose nanocrystal nanocomposite hydrogels. *Chemical Engineering Journal*. 2014 Sep;251:17–24. DOI: <https://doi.org/10.1016/j.cej.2014.04.034>.
32. Yang Z, Yang H, Jiang Z, Cai T, Li H, Li H, et al. Flocculation of both anionic and cationic dyes in aqueous solutions by the amphoteric grafting flocculant carboxymethyl chitosan-graft-polyacrylamide. *Journal of Hazardous Materials*. 2013 Jun;254–255:36–45. DOI: <https://doi.org/10.1016/j.jhazmat.2013.03.053>.
33. Wei X, Tao J, Li M, Zhu B, Li X, Ma Z, et al. Polyacrylamide-based inorganic hybrid flocculants with self-degradable property. *Materials Chemistry and Physics*. 2017 May;192:72–7. DOI: <https://doi.org/10.1016/j.matchemphys.2017.01.064>.
34. Yang F, Li G, He Y-G, Ren F-X, Wang G. Synthesis, characterization, and applied properties of carboxymethyl cellulose and polyacrylamide graft copolymer. *Carbohydrate Polymers*. 2009 Aug;78(1):95–9. DOI: <https://doi.org/10.1016/j.carbpol.2009.04.004>.
35. Ismi I, Rifi E, Lebkiri A, Oudda H. Spectral characterization of PA–Cu under two polymeric forms and their complex PA–Cu. *J Mater Environ Sci*. 2015;6(2):343–8.
36. Vijayalakshmi K, Devi BM, Latha S, Gomathi T, Sudha PN, Venkatesan J, et al. Batch adsorption and desorption studies on the removal of lead (II) from aqueous solution using nanochitosan/sodium alginate/microcrystalline cellulose beads. *International Journal of Biological Macromolecules*. 2017 Nov;104:1483–94. DOI: <https://doi.org/10.1016/j.ijbiomac.2017.04.120>.
37. Anirudhan TS, Unnithan MR, Divya L, Senan P. Synthesis and characterization of polyacrylamide-grafted coconut coir pith having carboxylate functional group and adsorption ability for heavy metal ions. *J Appl Polym Sci*. 2007 Jun 15;104(6):3670–81. DOI: <https://doi.org/10.1002/app.25002>.
38. Zendejdel M, Barati A, Alikhani H. Removal of heavy metals from aqueous solution by poly(acrylamide-co-acrylic acid) modified with porous materials. *Polym Bull*. 2011 Jul;67(2):343–60. DOI: <https://doi.org/10.1007/s00289-011-0464-5>.
39. Li N, Bai R, Liu C. Enhanced and Selective Adsorption of Mercury Ions on Chitosan Beads Grafted with Polyacrylamide via Surface-Initiated Atom Transfer Radical Polymerization. *Langmuir*. 2005 Dec;21(25):11780–7. DOI: <https://doi.org/10.1021/la051551b>.
40. Cao J, Tan Y, Che Y, Xin H. Novel complex gel beads composed of hydrolyzed polyacrylamide and chitosan: An effective adsorbent for the removal of heavy metal from aqueous solution. *Bioresource Technology*. 2010 Apr;101(7):2558–61. DOI: <https://doi.org/10.1016/j.biortech.2009.10.069>.
41. Payne KB, Abdel-Fattah TM. Adsorption of Divalent Lead Ions by Zeolites and Activated Carbon: Effects of pH, Temperature, and Ionic Strength. *Journal of Environmental Science and Health, Part A*. 2004 Dec 27;39(9):2275–91. DOI: <https://doi.org/10.1081/ESE-200026265>.
42. Xiao Y, Xue Y, Gao F, Mosa A. Sorption of heavy metal ions onto crayfish shell biochar: Effect of pyrolysis temperature, pH and ionic strength. *Journal of the Taiwan Institute of Chemical Engineers*. 2017 Nov;80:114–21. DOI: <https://doi.org/10.1016/j.jtice.2017.08.035>.
43. El-Bayaa AA, Badawy NA, AlKhalik EA. Effect of ionic strength on the adsorption of copper and chromium ions by vermiculite pure clay mineral. *Journal of Hazardous Materials*. 2009 Oct 30;170(2–3):1204–9. DOI: <https://doi.org/10.1016/j.jhazmat.2009.05.100>.
44. Yu B, Zhang Y, Shukla A, Shukla SS, Dorris KL. The removal of heavy metals from aqueous solutions by sawdust adsorption – removal of lead and comparison of its adsorption with copper. *Journal of Hazardous Materials*. 2001 Jun;84(1):83–94. DOI: [https://doi.org/10.1016/S0304-3894\(01\)00198-4](https://doi.org/10.1016/S0304-3894(01)00198-4).
45. Deniz F, Saygideger SD. Investigation of adsorption characteristics of Basic Red 46 onto gypsum: Equilibrium, kinetic and thermodynamic studies. *Desalination*. 2010 Nov;262(1–3):161–5. DOI: <https://doi.org/10.1016/j.desal.2010.05.062>.
46. Ouass A, Ismi I, Elaidi H, Lebkiri A, Cherkaoui M, Rifi E. Mathematical Modeling Of The Adsorption Of Trivalent Chromium By The Sodium Polyacrylate Beads. *J Mater Environ Sci*. 2017;8:3448–56.
47. Largitte L, Pasquier R. A review of the kinetics adsorption models and their application to the adsorption of lead by an activated carbon. *Chemical Engineering Research and Design*. 2016 May;109:495–504. DOI: <https://doi.org/10.1016/j.cherd.2016.02.006>.

48. Sekar M, Sakthi V, Rengaraj S. Kinetics and equilibrium adsorption study of lead(II) onto activated carbon prepared from coconut shell. *Journal of Colloid and Interface Science*. 2004 Nov;279(2):307-13. DOI: <https://doi.org/10.1016/j.jcis.2004.06.042>.
49. Robati D. Pseudo-second-order kinetic equations for modeling adsorption systems for removal of lead ions using multi-walled carbon nanotube. *J Nanostruct Chem*. 2013 Dec;3(1):55. DOI: <https://doi.org/10.1186/2193-8865-3-55>.
50. Özacar M, Şengil İA, Türkmenler H. Equilibrium and kinetic data, and adsorption mechanism for adsorption of lead onto valonia tannin resin. *Chemical Engineering Journal*. 2008 Sep;143(1-3):32-42. DOI: <https://doi.org/10.1016/j.cej.2007.12.005>.
51. Rathinam A, Maharshi B, Janardhanan SK, Jonnalagadda RR, Nair BU. Biosorption of cadmium metal ion from simulated wastewaters using *Hypnea valentiae* biomass: A kinetic and thermodynamic study. *Bioresource Technology*. 2010 Mar;101(5):1466-70. DOI: <https://doi.org/10.1016/j.biortech.2009.08.008>.
52. Fifi U, Winiarski T, Emmanuel E. Assessing the Mobility of Lead, Copper and Cadmium in a Calcareous Soil of Port-au-Prince, Haiti. *IJERPH*. 2013 Nov 4;10(11):5830-43. DOI: <https://doi.org/10.3390/ijerph10115830>.
53. Gomes PC, Fontes MPF, da Silva AG, de S. Mendonça E, Netto AR. Selectivity Sequence and Competitive Adsorption of Heavy Metals by Brazilian Soils. *Soil Sci Soc Am J*. 2001 Jul;65(4):1115-21. DOI: <https://doi.org/10.2136/sssaj2001.6541115x>.
54. Yan WL, Bai R. Adsorption of lead and humic acid on chitosan hydrogel beads. *Water Research*. 2005 Feb;39(4):688-98. DOI: <https://doi.org/10.1016/j.watres.2004.11.007>.
55. Ju X-J, Zhang S-B, Zhou M-Y, Xie R, Yang L, Chu L-Y. Novel heavy-metal adsorption material: ion-recognition P(NIPAM-co-BCAm) hydrogels for removal of lead(II) ions. *Journal of Hazardous Materials*. 2009 Aug 15;167(1-3):114-8. DOI: <https://doi.org/10.1016/j.jhazmat.2008.12.089>.
56. Yao Q, Xie J, Liu J, Kang H, Liu Y. Adsorption of lead ions using a modified lignin hydrogel. *J Polym Res*. 2014 Jun;21(6):465. DOI: <https://doi.org/10.1007/s10965-014-0465-9>.
57. Sun Y, Ma Y, Fang G, Li S, Fu Y. Synthesis of Acid Hydrolysis Lignin-g-Poly-(Acrylic Acid) Hydrogel Superabsorbent Composites and Adsorption of Lead Ions. *BioResources*. 2016 May;11(3):5731-42. URL: <https://ojs.cnr.ncsu.edu/index.php/BioRes/article/view/7960>.
58. Mohammadinezhad A, Marandi GB, Farsadrooh M, Javadian H. Synthesis of poly(acrylamide-co-itaconic acid)/MWCNTs superabsorbent hydrogel nanocomposite by ultrasound-assisted technique: Swelling behavior and Pb (II) adsorption capacity. *Ultrasonics Sonochemistry*. 2018 Dec;49:1-12. DOI: <https://doi.org/10.1016/j.ultsonch.2017.12.028>.
59. Bulut Y, Akçay G, Elma D, Serhatlı IE. Synthesis of clay-based superabsorbent composite and its sorption capability. *Journal of Hazardous Materials*. 2009 Nov;171(1-3):717-23. DOI: <https://doi.org/10.1016/j.jhazmat.2009.06.067>.

